Front. Optoelectron. China 2011, 4(2): 181–187
DOI 10.1007/s12200-011-0162-9

RESEARCH ARTICLE

Controllable synthesis of quasi-spherelike ZnO hierarchical nanostructures and performance of their dye-sensitized solar cells

Yanhua TONG (✉), Feng CAO, Peisong TANG, Haifeng CHEN, Guoxiang PAN, Minhong XU

Department of Chemistry, Huzhou Teachers College, Huzhou 313000, China

Abstract Hierarchical zinc oxide (ZnO) quasi-spheres consisting of nanoparticles with diameter of about 20 nm were synthesized via a one-pot reaction. The size of ZnO quasi-spheres is easily tunable from 80 nm to 3 μm by varying the type of zinc source and its concentration. The three samples 1–3 with the diameter of 80–180 nm, 300–600 nm and 1.2–2.9 μm were selected for fabricating dye-sensitized solar cells (DSSCs) and their photovoltaic properties were measured. The results demonstrate that DSSCs fabricated by sample 2 with the diameter within the wavelength of visible light obtain the highest short-circuit current density and over light conversion efficiency, due to resonant scattering increasing the photon absorption.

Keywords zinc oxide, quasi-spheres, dye-sensitized solar cells, photovoltaic property

1 Introduction

Monodisperse colloidal microspheres with controlled size are of key importance in colloidal chemistry and material chemistry because of the theoretical research on them in physical chemistry and their potential applications in optics, electronics, catalysis, sensors, and so forth [1–4]. Moreover, recent work on the crystallization of colloidal spheres has fully demonstrated the potential to obtain interesting and useful functionality not only from the constituent materials of the colloidal particles but also from the long-range order of the crystalline lattice [5–10]. As a result, much effort has been devoted to the synthesis of colloidal spheres of various materials, such as polystyrene [11], silica [12], ZnSe [13–17], ZnS [18–20], CdS [21], CdSe [22], Ag_2Se [23], TiO_2 [24–26], ZnO [27,28], PbS [29].

Received November 15, 2010; accepted November 30, 2010

E-mail: tyh@hutc.zj.cn

However, the reported colloidal spheres of semiconductors have mainly been synthesized by template-directed approach, in which the easy-fabrication colloidal spheres of materials are used as the template and are then coated or reacted with other materials. This is because semiconductors tend to grow anisotropically into non-spherical structures, including rods, wires, belts, tetrapods, cubes, and flowers. Hence, it is still a challenge to fabricate spherelike inorganic semiconductors in large quantities by a simple direct synthesis.

As an important II–VI semiconductor with a wide and direct band gap (3.37 eV) and a large exciton binding energy (60 eV), ZnO will attract much interest in the field of colloidal materials, owing to its specific electrical, catalytic, photochemical and optoelectronic properties [30–32]. Zhang's group reported that ZnO colloid spheres synthesized by refluxing in diethylene glycol display good photovoltaic properties [33].

Here, ZnO quasi-spherelike colloids were synthesized by aqueous precipitate, using zinc salts and diethanolamine (DEA) as raw materials. The size of quasi-spherelike colloids can be modulated in the range of 80 nm–3 μm by adjusting starting concentration of zinc source, solvents, and electrolytes. The measurements of photovoltaic properties of different-size ZnO spheres demonstrate that quasi-spheres of 300–600 nm have the highest short-circuit current density (J_{sc}) and over light conversion efficiency (η). This result should be attributable to the resonant scattering existing in the quasi-spheres with the wavelength of the visible light, leading to the enhancement of photon absorption.

2 Experimental details

2.1 Synthetic procedures

All the chemical reagents used in our experiments were of analytical grade and used as received. $Zn(NO_3)_2 \cdot 6H_2O$

(0.005 mol) was dissolved in deionized water (70 mL) under magnetic stirring and then DEA (30 mL, 98%) was added to form a transparent mixture. The same procedures were repeated to prepare the mixture with various starting concentration of zinc salts and solvents. Subsequently, such mixture was transferred to a two-necked flask and refluxed at 110°C for 2 h. A large quantity of white precipitates at the bottom of flask were collected and washed with alcohol and de-ionized water several times. The residues were then dried at 60°C in an oven for 3 h.

2.2 Characterization

The phase and crystal structure of the products were determined by X-ray diffraction (XRD, Siemens D-500 with Cu Kα radiation and normal 2θ scans). The morphology and microstructure of the sample were analyzed by scanning electron microscopy (SEM; JEOL JSM-820) and field emission scanning electron microscopy (FESEM; JEOL JSM-63357). The specific surface area was measured by a BET Surface Area Analyzer (Coulter products SA3100).

2.3 Preparation of ZnO film electrodes and measurement of dye-sensitized solar cells (DSSCs)

To fabricate ZnO films, the conductive glass substrates were first cleaned by sonicating in detergent, acetone and ethanol in order and then air-dried. Parallel edges of each substrate were covered with 10 μm-thick scotch tape to control the thickness of the film. A few drops of the resultant ZnO colloidal spheres were then placed onto the glass substrates and the films were formed by a doctor-blading process. The films were then immediately heated at a temperature of 350°C for 1 h, forming a layer of white film during the quick evaporation of the solvent. The thickness of the film is estimated to be 10 μm, which is the similar thickness as the spacers.

Before solar cell testing, the ZnO films were heated to 70°C and sensitized with standard ruthenium-based N_3 red dye. The heated films were immersed in N_3 dye with a concentration of 5×10^{-4} M in ethanol for 20 min. The samples were then rinsed with ethanol to remove excess dye on the surface and air-dried at room temperature. The counter electrode consisting of a platinum-coated silicon substrate was face to face placed on the ZnO film electrode. The two electrodes were then sandwiched together with two heavy duty clips.

The electrolyte in this study was a liquid admixture containing 0.5 M LiI, 50 mM I_2, and 0.5 M 4-tertbutylpyridine in 3-methoxypropionitrile. The photovoltaic behavior was characterized when the cell devices were irradiated by simulated AM 1.5 sunlight with an output power of 100 $mW\cdot cm^{-2}$. An Ultraviolet Solar Simulator (Oriel 66902) with a 200 W Xenon Lamp Power Supply was used as the light source, and a Semiconductor Parameter Analyzer was used to measure current-voltage (*I-V*) curves.

3 Results and discussion

The morphology and size distribution of the as-prepared samples were investigated using the SEM technique. Figure 1 shows the SEM images of three typical samples prepared by refluxing within different parameters. The low-magnification SEM images in Figs. 1(a), 1(c) and 1(e) display a quasi-spherelike shape over a large area from sample 1, sample 2 and sample 3, respectively. The high-magnification SEM images in Figs. 1(b), 1(d) and 1(f) show the sizes of the quasi-spheres in sample 1, sample 2 and sample 3, respectively. The results demonstrate that the size of quasi-spheres can be modulated by varying Zn^{2+} source and its concentration. The details of size distribution were analyzed by histograms in Fig. 2, which are depicted via measuring the diameters of the quasi-spheres in SEM images (Each sample was randomly selected 250 particles out). It is followed that the diameter of sample 1 is among 80–180 nm, sample 2 among 300–600 nm, sample 3 among 1.3–2.9 μm. This result shows that the size distribution of the as-prepared samples is broad.

To analyze the detailed structure of the as-prepared quasi-spheres, high-magnification FESEM were used. Figures 3(a) and 3(b) show the FESEM images of samples prepared via a $Zn(NO_3)_2\cdot6H_2O$-H_2O system and $Zn(CH_3COO)_2\cdot2H_2O$-C_2H_5OH system, respectively, both displaying hierarchical nanostructures. The typical quasi-spheres are the aggregates of smaller particles of about dozens of nanometer in diameter.

Figure 4 shows the XRD patterns acquired from the three samples. All of the diffraction peaks of each sample were indexed as a hexagonal phase of wurtize-type ZnO, consistent with JCPDS card No. 36–1451. No other impurities, such as $Zn(NO_3)_2$, $Zn(OH)_2$, and other compounds were detected. The clearness and high intensity of diffraction peaks in the XRD pattern confirm that the products are well-crystallized. The width of diffraction peaks indicates that the as-prepared quasi-spheres are composed of small nanoparticles, which is in accord with the high-magnification FESEM observations. On the full width at half-maximum (FWHMs) of (100), (002) and (101) diffraction peaks, the average sizes of constructing subunits of the as-prepared ZnO quasi-spheres were calculated according to the Scherrer equation [34] and the results are shown in Table 1. The average sizes of the subunits of sample 1, sample 2 and sample 3 are 21, 19 and 22 nm, respectively.

The surface area and total pore volume of the ZnO quasi-spheres were measured by nitrogen sorption isotherms (the relative error of the used machine is smaller than 2% for the high speed gas sorption analyzer). The data were summarized in Table 2. Sample 2 has the largest BET

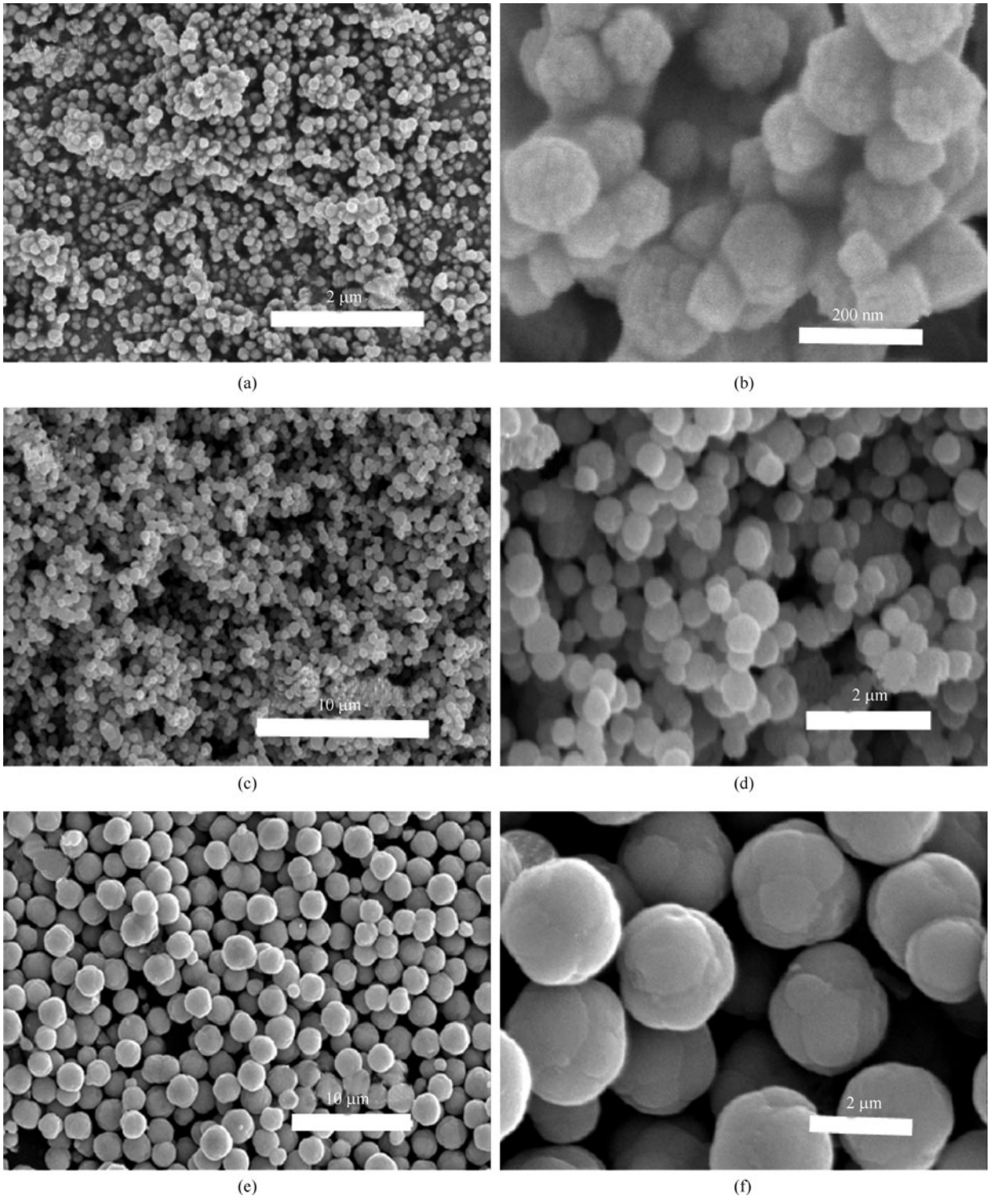

Fig. 1 SEM images of three typical ZnO quasi-spheres prepared by refluxing under different parameters. (a) and (b) 1 g of $Zn(CH_3COO)_2 \cdot 2H_2O$ dissolved into the mixture of 110 mL ethanol and 2.5 mL DEA (sample 1); (c) and (d) 2.25 g of $Zn(NO_3)_2 \cdot 6H_2O$ dissolved into the mixture of 80 mL H_2O and 30 mL DEA (sample 2); (e) and (f) 1.5 g of $Zn(NO_3)_2 \cdot 6H_2O$ dissolved into the mixture of 80 mL H_2O and 30 mL DEA (sample 3)

surface area. With regard to the total pore volume of samples, it is getting smaller in the order of samples 1–3. On the basis of this result, it can be followed that the aggregation of subunits for the samples is more and more compact. Therefore, the compactness for samples 1–3 is getting better in sequence.

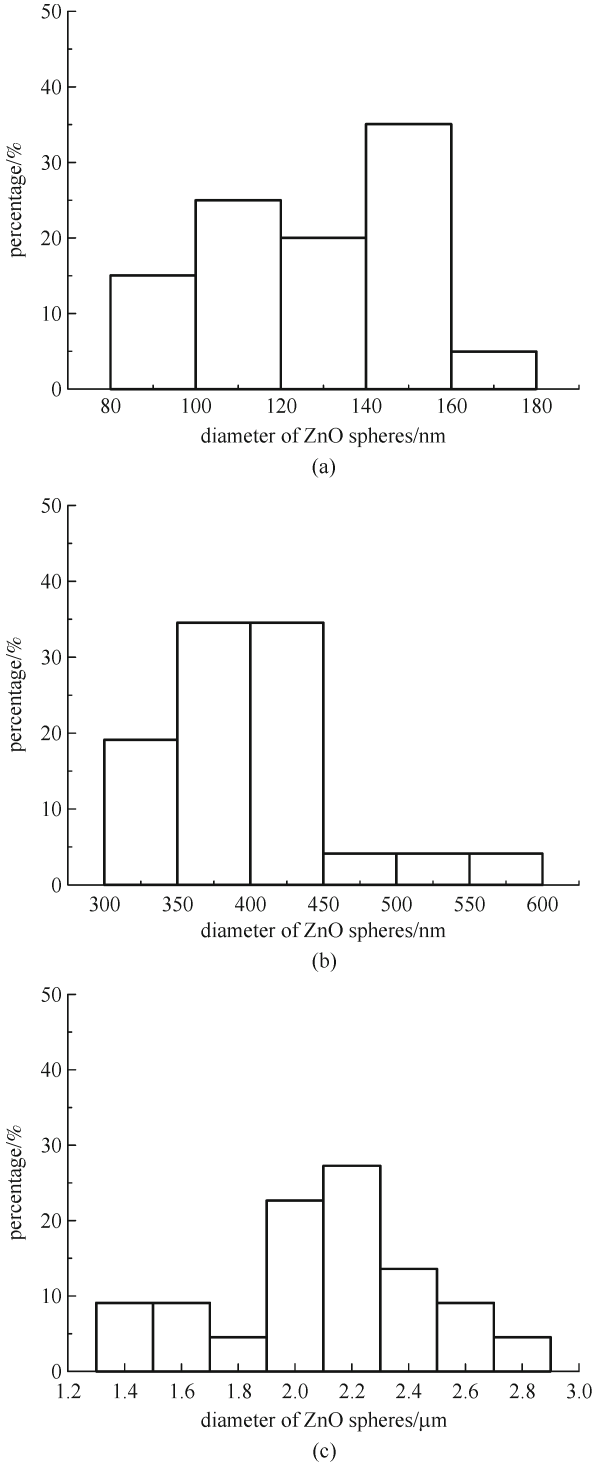

Fig. 2 Diameter distribution of the as-prepared ZnO quasi-spheres. (a) Sample 1; (b) sample 2; (c) sample 3

The three solar cells fabricated with different-size ZnO quasi-spheres (samples 1–3) were characterized by measuring *I-V* behavior when the cells were irradiated with a power density of $100\,\mathrm{mW\cdot cm^{-2}}$ and in dark. The corresponding current density *J-V* curves were shown in Fig. 5. Table 3 summarizes the measured and calculated values of the cells' parameters acquired from each *J-V* curve in Fig. 5(a), including J_{sc}, open-circuit voltage (V_{oc}), maximum voltage (V_{max}) out, maximum current (J_{max}) out, filled factor (FF), η. It clearly shows that sample 2 achieves the highest J_{sc} and η, whereas sample 3 is the lowest. All the samples possess the similar V_{oc} of approximately 600 mV and dark *J* before bias *V* of 600 mV.

In a DSSC, the V_{oc} is dependent on the potential difference established by the *V* of the film and that of the Pt counter electrode, in which, the surface chemistry of the film's material may influence the V_{oc}. Since the three solar cells are fabricated with the similar materials and the same procedures. The similar V_{oc} for them is expected. The J_{sc} is determined by the initial number of photogenerated carriers, the injection efficiency of electrons from dye molecules to semiconductor, and the recombination rate between the injected electrons and oxidized dye or redox species in the electrolyte. It is reasonable to assume the same injection efficiency and recombination rate for the given ZnO/N_3/electrolyte systems. Accordingly, the initial number of photogenerated carriers may be significantly affected by the variation in the light-harvesting capability of photoelectrodes with different film structures. In the three fabricated DSSCs, the only difference between them is the diameter of ZnO quasi-spheres for the three samples, which may lead to the difference of the J_{sc} between them. The specific explanation is as follows.

Typically, light scattering [35] occurs with particle $>$100 nm in diameter. Further, Mie theory [36] and Anderson localization of light [37] provide the analytical description for the scattering of light by spherical particles and predict that resonant scattering may occur when the particle size is comparable to the wavelength of incident light. The secondary quasi-spheres for sample 2 are 300–600 nm in diameter and within the wavelength of visible light. They can therefore become efficient scatterers for visible light and even produce resonant scattering in the DSSC, which results in an increase in the generation of electron-hole pairs and light-harvesting capability of the photoelectrode. The J_{sc} and η are enhanced in the DSSC fabricated from sample 2. However, samples 1 and 3 are nano-sized and micrometer-sized, respectively, which are far from the wavelength of visible light. Hence, they can not produce resonant scattering and obtain a relatively low J_{sc} and η.

The three samples possess a similar FF in Table 3. The FF in a DSSC is affected by the capability of inhibition of the back electron transfer from ZnO to I_3^- [38]. If ZnO film has a high connectivity between subunits, there is a rapid collection of photogenerated electrons and the degree of charge recombination get reduced so as to enhance the FF. The samples 1–3 get more and more compact in sequence as the above-mentioned discussion, leading to higher and higher FF value in the same sequence. However, the FF in this work is lower than the previous reports [33,39,40]. The polydisperse of the as-prepared ZnO quasi-spheres may have caused incomplete particle packing and cracking after

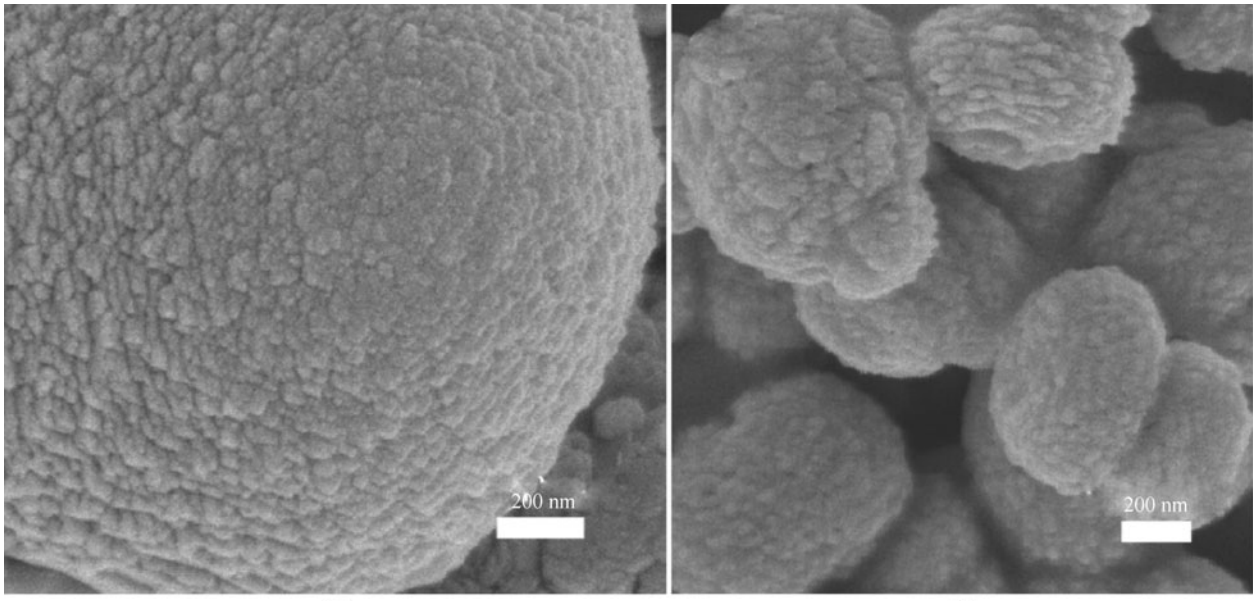

Fig. 3 FESEM images of ZnO quasi-spheres prepared via different systems. (a) $Zn(NO_3)_2 \cdot 6H_2O$-H_2O system; (b) $Zn(CH_3COO)_2 \cdot 2H_2O$-$C_2H_5OH$ system

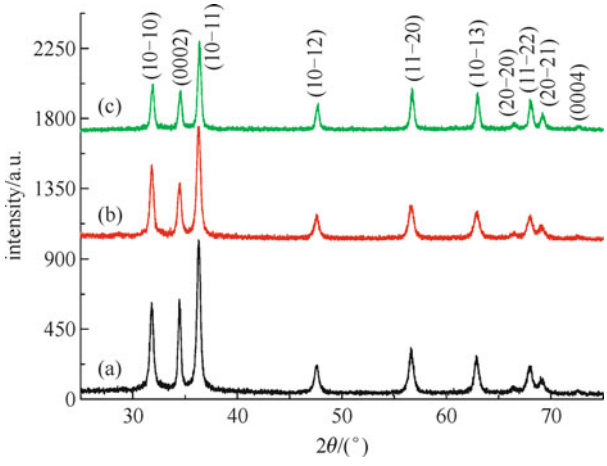

Fig. 4 XRD characterization of as-prepared ZnO samples. (a) Sample 1; (b) sample 2; (c) sample 3

Table 1 Size of component nanoparticles of three samples calculated from XRD peaks

diffraction peak	sample 1	sample 2	sample 3
(100)	22.313±0.002	19.774±0.002	22.372±0.002
(002)	20.062±0.002	20.051±0.002	22.221±0.002
(101)	22.581±0.002	18.042±0.002	22.271±0.002
average/nm	21.322±0.002	19.292±0.002	22.291±0.002

sintering, which would result in low connectivity among quasi-spheres and influence the FF in a DSSC.

Table 2 BET surface areas and total pore volumes of three ZnO samples with different sizes

sample	BET surface area/($m^2 \cdot g^{-1}$)	total pore volume/(ccg^{-1})
1	12.62	6.07×10^{-2}
2	14.88	3.64×10^{-2}
3	2.04	4.23×10^{-3}

4 Conclusion

In this paper, ZnO quasi-spheres, aggregated nanoparticles with about 20 nm in diameter, were synthesized via a simple and low-temperature aqueous solution route. The size of ZnO quasi-spheres is easily tunable from dozens of nanometer to several micrometers by changing the type and concentration of zinc salts. The DSSCs constructed by ZnO quasi-spheres of 300–600 nm in diameter obtain the highest J_{sc} and η, compared to other samples with the diameter of 80–180 nm and 1.3–2.9 μm. The improvement of J_{sc} and η for sample 2 should be attributable to the resonant scattering produced in the photoelectrode that can enhance the light-harvesting capability. Although the property of DSSCs fabricated from the as-fabricated ZnO quasi-spheres is inferior to other reports, it indirectly confirms that the resonant scattering exists only in particles with the diameter of the wavelength of visible light.

Acknowledgements The work was financially supported by the Zhejiang Province Natural Science Foundation (Nos. Y4100471 and Y4110641) and the Science and Technology Planning Project of Zhejiang Province (No. 2008F70042).

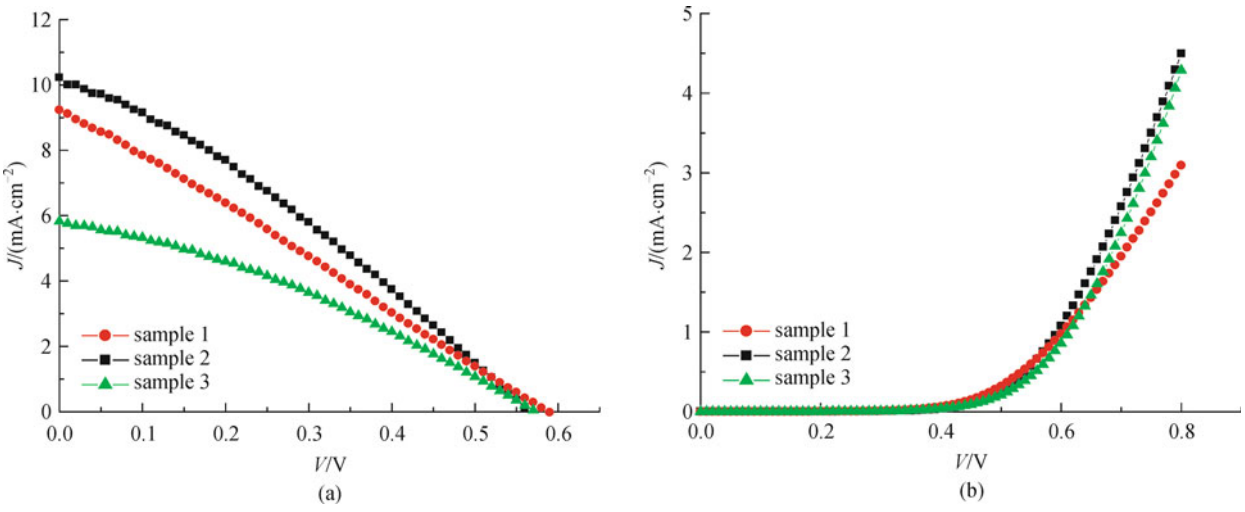

Fig. 5 *J-V* characteristics for solar cells constructed by different-size ZnO quasi-spheres. (a) Under illumination; (b) in dark

Table 3 Photovoltaic properties of DSSCs based on different-size ZnO spheres

ZnO film	V_{oc}/mV	J_{sc}/(mA·cm^{-2})	V_{max}/mV	J_{max}/(mA·cm^{-2})	FF[1)]/%	η[1)]/%
sample 1	584	9.2	300	4.8	26.5	1.42
sample 2	564	10.2	300	5.8	30.2	1.74
sample 3	568	5.8	310	3.6	33.2	1.1

1) η and FF are calculated from $\eta = P_{out,\,max}P_{in}^{-1}$ and $FF = P_{out,\,max}(V_{oc}J_{sc})^{-1}$, where $P_{out,\,max}$ is the maximum output power density, P_{in} is the incident light power density, V_{oc} is the photovoltage at open circuit

References

1. Matijevic E. Monodipersed colloid-art and scicence. Langmuir, 1986, 2(1): 12–20
2. Matijevic E. Preparation and properties of uniform size colloids. Chemistry of Materials, 1993, 5(4): 412–426
3. Matijevic E. Uniform inorganic colloid dispersions — achievement and challenges. Langmuir, 1994, 10(1): 8–16
4. Jeong U, Wang Y L, Ibisate M, Xia Y N. Some new developments in the synthesis, functionalization, and utilization of monodisperse colloidal spheres. Advanced Functional Materials, 2005, 15(12): 1907–1921
5. Velev O D, Lenhoff A M. Colloidal crystals as templates for porous materials. Current Opinion in Colloid & Interface Science, 2000, 5 (1–2): 56–63
6. Stein A, Schroden R C. Colloidal crystal templating of three-dimensionally ordered macroporous solid: materials for photonics and beyond. Current Opinion Solid State & Materials Science, 2001, 5(6): 553–564
7. Polman A, Wiltzius P. Materials science aspects of photonic crystals. MRS Bulletin, 2001, 26(8): 608–610
8. Vlasov Y A, Bo X Z, Sturm J C, Norris D J. On-chip natural assembly of silicon photonic bandgap crystals. Nature, 2001, 414 (6861): 289–293
9. Lee W M, Prunziski S A, Braun P V. Multi-photon polymerization of waveguide structures within three-dimensional photonic crystals. Advanced Materials, 2002, 14(4): 271–274
10. López C. Materials aspects of photonic crystals. Advanced Materials, 2003, 15(20): 1679–1704
11. Arshady R. Suspension, emulsion, and dispersion polymerization — a methodological survey. Colloid and Polymers Science, 1992, 270 (8): 717–732
12. Stöber W, Fink A, Bohn E. Controlled growth of monodisperse silica spheres in micron size range. Journal of Colloid and Interface Science, 1968, 26(1): 62–69
13. Peng Q, Dong Y J, Li Y D. ZnSe semiconductor hollow microspheres. Angewandte Chemie — International Edition, 2003, 42(26): 3027–3030
14. Yao W T, Yu S H, Jiang J, Zhang L. Complex wurtzite ZnSe microspheres with high hierarchy and their optical properties. Chemistry — A European Journal, 2006, 12(7): 2066–2072
15. Jiang C L, Zhang W Q, Zou G F, Yu W C, Qian Y T. Synthesis and characterization of ZnSe hollow nanospheres via a hydrothermal route. Nanotechnology, 2005, 16(4): 551–554
16. Shen G Z, Chen D, Tang K B, Qian Y T. Characterization of ZnSe spheres via a rapid polyol process. Journal of Crystal Growth, 2003, 257(3–4): 276–279
17. Zhong H Z, Wei Z X, Ye M F, Yan Y, Zhou Y, Ding Y Q, Yang C H, Li Y F. Monodispersed ZnSe colloidal microspheres: preparation, characterization, and their 2D arrays. Langmuir, 2007, 23(17): 9008–9013
18. Murphy-Wilhelmy D, Matijevic E. Preparation and properties of monodispersed spherical-colloidal particles of zinc sulfide. Journal of the Chemical Society — Faraday Transactions. 1984, 80: 563–

570

19. Velikov K P, Van B A. Synthesis and characterization of monodisperse core-shell colloidal spheres of zinc sulfide and silica. Langmuir, 2001, 17(16): 4779–4786
20. Breen M L, Dinsmore A D, Pink R H, Qadri S B, Ratna B R. Sonochemically produced ZnS-coated polystyrene core-shell particles for use in photonic crystals. Langmuir, 2001, 17(3): 903–907
21. Matijevic E, Murphy-Wilhelmy D. Preparation and properties of monodispersed spherical colloidal particles of cadmium. Journal of Colloid and Interface Science, 1982, 86(2): 476–484
22. Jeong U, Kim J U, Xia Y N. Monodispersed spherical colloids of Se@CdSe: synthesis and use as building blocks in fabricating photonic crystals. Nano Letter, 2005, 5(5): 937–942
23. Jeong U, Xia Y N. Photonic crystals with thermally switchable stop bands fabricated from Se@Ag_2Se spherical colloids. Angewandte Chemie — International Edition, 2005, 44(20): 3099–3103
24. Jiang X C, Herricks T, Xia Y N. Monodispersed spherical colloids of titania: synthesis, characterization, and crystallization. Advanced Materials, 2003, 15(14): 1205–1209
25. Zhong Z Y, Yin Y D, Gates B, Xia Y N. Preparation of mesoscale hollow spheres of TiO_2 and SnO_2 by templating against crystalline arrays of polystyrene beads. Advanced Materials, 2000, 12(3): 206–209
26. Yin Y D, Lu Y, Gates B, Xia Y N. Synthesis and characterization of mesoscopic hollow spheres of ceramic materials with functionalized interior surfaces. Chemistry of Materials, 2001, 13(4): 1146–1148
27. Jezequel D, Guenot J, Jouini N, Fievet F. Preparation and morphological characterization of fine, spherical, monodisperse particles of ZnO. Materials Science Forum, 1994, 152–153: 339–342
28. Xu S, Li Z H, Wang Q, Cao L J, He T M, Zou G T. A novel one-step method to synthesize nano/micron-sized ZnO sphere. Journal of Alloys and Compounds, 2008, 465(1–2): 56–60
29. Wang Y L, Cai L, Xia Y N. Monodisperse spherical colloids of Pb and their use as chemical templates to produce hollow particles. Advanced Materials, 2005, 17(4): 473–477
30. Joo J, Kwon S G, Yu J H, Hyeon T. Synthesis of ZnO nanocrystals with cone, hexagonal cone, and rod shapes via non-hydrolytic ester elimination sol-gel reactions. Advanced Materials, 2005, 17(15): 1873–1877
31. Pal U, Santiago P. Controlling the morphology of ZnO nanostructures in a low-temperature hydrothermal process. Journal of Physical Chemistry B, 2005, 109(32): 15317–15321
32. Vayssieres L. Growth of arrayed nanorods and nanowires of ZnO from aqueous solutions. Advanced Materials, 2003, 15(5): 464–466
33. Zhang Q F, Chou T R, Russo B, Jenekhe S A, Cao G Z. Aggregation of ZnO nanocrystallites for high conversion efficiency in dye-sensitized solar cells. Angewandte Chemie — International Edition, 2008, 47(13): 2402–2406
34. Cullity B D. Elements of X-Ray Diffraction. 2nd ed. Massachusetts: Addison-Wesley, 1956
35. Cao G Z. Nanostructures & Nanomaterials: Synthesis, Properties, & Applications. London: Imperial College Press, 2004
36. Hulst H C. Light Scattering by Small Particles. New York: Wiley, 1957
37. Wolf P E, Maret G. Weak localization and coherent backscattering of photons in disordered media. Physical Review Letter, 1985, 55 (24): 2696–2699
38. Kay A, Grätzel M. Dye-sensitized core-shell nanocrystals: improved efficiency of mesoporous tin oxide electrodes coated with a thin layer of an insulating oxide. Chemistry of Materials, 2002, 14(7): 2930–2935
39. Jiang C Y, Sun X W, Lo G Q, Kwong D L. Improved dye-sensitized solar cells with a ZnO-nanoflower photoanode. Applied Physics Letters, 2007, 90(26): 263501
40. Pradhan B, Batabyal S K, Pal A J. Vertically aligned ZnO nanowire arrays in Rose Bengal-based dye-sensitized solar cells. Solar Energy Materials & Solar Cells, 2007, 91(9): 769–773